4th Intercontinental Geoinformation Days

Modeling of land subsidence in Shabestar Plain and its relation to groundwater by radar interferometry

Naghmeh Mousakhani [*1] **Khalil Valizadeh Kamran[1]**

1University of Tabriz, Faculty of Planning and Environmental Sciences, Department of Remote Sensing and GIS, Tabriz, Iran

Keywords
Land subsidence
Radar interferometry
Groundwater
Moran index
Shabestar Plain

Abstract
Shabestar plain has been faced the phenomenon of gradual subsidence in recent years and it is one of the most important plains in East Azerbaijan province in terms of agricultural lands. In this research, the radar interferometry interferogram time series analysis was used in order to predict the subsidence centers of the plain and InSAR data of Sentinel 1as satellite was employed for measuring land subsidence in Shabestar plain with high spatial and temporal resolution in the period 2015-2019 and Adaptive filter was used to modify and refine the phase in each of the images. The result of radar interferometry showed a significant subsidence in the center and west of Shabestar plain with a subsidence rate of 24 cm in this interval. The subsidence level of groundwater level was about 16 m^3 measured with Kriging tool. The spatial analysis technique and Moran index of 98% and P value of zero depicted a strong relationship between land subsidence and groundwater level. Unauthorized wells with more exploitation and consequent change of land use and geological conditions in this plain have increased the rate of land subsidence and implementation of the plans for reduction of the risks of land subsidence seems essential.

1. Introduction

In recent years, with domination of dry climate in most parts of Iran and concentration of increasing agricultural exploitation of drinking water and industrial groundwater resources have provided the necessary infrastructure for this phenomenon that is a serious crisis in many plains of the country.

Shabestar plain is located in East Azerbaijan province in the north of Tabriz plain and on the southern slopes of Mishu mountain. This plain is located on 60 km from the city of Tabriz and is one of the 25 sub-basins of Lake Urmia "Fig. 1".

According to the USGS database, more than 100 recorded subsidence factors are related to groundwater (USGS 2014). As a result of reaction to the quality and quantity of groundwater in the surface aquifer, two environmental phenomena of subsidence and settlement can be mentioned which are usually associated with the dissolution of bedrock and gradual sinking of the surface (Ford and William 2007).
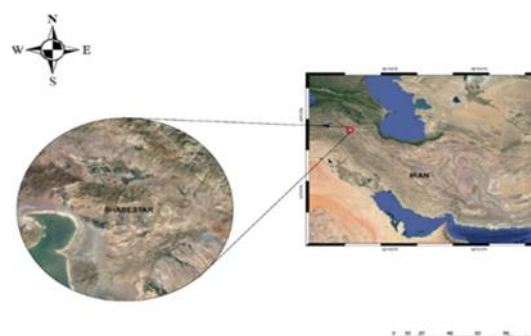

Figure 1. Location map of the studied area in Iran

The use of InSAR technique for detection and monitoring long-term movements has been well proven in the last decade for various types of landslides and subsidence due to its vast spatial coverage, high spatial and temporal resolution, operational capability and

Cite this study

Mousakhani, N., Kamran, K. V. (2022). Modeling of land subsidence in Shabestar Plain and its relation to groundwater by radar interferometry. 4th Intercontinental Geoinformation Days (IGD), 118-121, Tabriz, Iran

weather conditions (Raucoles et al. 2020) (Vietmeier et al. 1999).

Since InSAR time series perform accurate mapping of land subsidence, the relationships between the geological fault subsidence and the groundwater level in the studied plain have been investigated to consider the evolution parameters of land subsidence. An interferogram is an image that contains a phase difference between two radar images that are geometrically recorded relative to each other (Daniel et al. 2003).

Subsidence phenomenon can cause superficial morphological effects such as morphological irregularities, damage to man-made buildings, highways and streets, agricultural water supply network and subsurface effects such as reduced aquifer volume (Chen et al. 2010; Galloway 1998).

If the site of subsidence is prone to other hazards such as earthquakes and floods, which can have catastrophic destructive effects, then monitoring the rate and extent of subsidence and measuring the changes and morphological effects in these areas can be an effective step in preventing and relative control of the phenomenon.

Severe subsurface subsidence has caused various adverse effects in Shabestar-Sufiyan plain, including reduction of water reservoir and drying of a number of wells, reduction of underground water quality and the occurrence of subsidence or downward movement in some areas.

2. Method

For processing, radar interferometry method with artificial valve and InSAR radar interferometry technique and Sar Map software Envi 5.3 have been used.

Differential radar interferometry calculates phase changes from two pairs of radar images taken at different times to quantitatively and qualitatively reveal these changes in the earth's crust (Ketelaar 2008). It was also used to remove the topographic effect from the USRS site SRTM digital elevation model.

Adaptive filter was used to filter the differential interferometers obtained from the previous step and to improve the quality of the interferometers. Adaptive algorithms have been applied to various problems such as noise cancellation, echo signal prediction, channel equalization and compatible presentations. Also, due to the real-time auto-tuning feature, an adaptive filter can be used to track the behavior of maximum variable slow signals (Haykin et al. 2007).

After phase correction and refinement of the results of interferogram by applying the phase-to-distance conversion factor, displacement rate maps were prepared in the period 2015-2019.

In addition, the groundwater level data belonging to the studied area were compared and evaluated in order to find the causes of subsidence in relation to the groundwater water level obtained in the well.

In this research, the use of SAR data of Sentinel S1a sensor in SLC form, uses polarization data of vv bands, is the slope angle and distance of azimuth meter. In addition, simulation of DEM topographic signal with coverage of the area has been used.

Although the Sentinel 1A provides bipolar data sources, the vertical transmission / vertical reception VV and its cross-pole receive horizontal reception. VH provides better VV data (Clement et al. 2018) (Twele et al. 2016).

InSAR technology is capable of producing large maps of about 10000 km3 (Sun et al. 2016). The selection of SAR images, one as a master and the other as a slave, has been downloaded from the Sentinel images site, which interferes with the pairing of two SAR images.

Calculation of the interferogram phase is done by the following equation:

An interferogram is calculated by multiplying the amplitude of two images and the phase difference.

Differences are created by distinguishing the phase value of two radar images obtained from different times in the same area (Karimzadeh and Ahmadi 2013). Some of these interactions have been selected to help the stack shift map (Wright et al. 2001) (Motagh et al. 2006) and (Walters et al. 2011).

The resulting images must have approximately the same geometry to be able to use coherent interferometry pairs used to generate digital elevation models, mapping and monitoring the deformation of the earth (Zebker 1992) (Gatelli et al. 1994).

In this regard, a phase change of 2π is equivalent to a displacement of half the wavelength used by the satellite, which represents a complete French in the interferogram.

The interferogram phase is created due to components such as orbital component, topography, displacement, atmosphere and noise that each of the parameters causes the phase change.

Relative position of a number of the terrestrial events changes slightly between the two SAR images, which is independent of the baseline. Therefore, the signals received from the structures and the road surface lead to the loss of coherence and the difference between the two synchronous image pairs is less than the coherent of the pre-event pair images.

The difference between the two images pairs can be calculated for plotting the affected areas (Ishitsuka et al. 2012) (Lu et al. 2018). These changes are resultant from subsidence, landslide and displacement of the faults.

After flatting d in the formula, interferometry phase interferogram will be according to following relation

$$\Delta\varphi = -\frac{4\pi}{\lambda}\frac{B_n q}{R \ \sin\Theta} + \frac{4\pi}{\lambda}$$

The obtained interferogram from this step is called differential interferogram and the remained phase is basically the result of the earth crust changes.

SRTM arc secdata topography with a resolution of 30 meters along with GCP points was used to eliminate topographic and atmospheric phases. For selecting GCP points, the coherent areas with smooth topography and away from shifted areas were identified.

In the last stage, the image was converted to the WGS84 global system and for analyzing its classification

in GIS software and its relationship with the groundwater level of the areas were determined.

2.1. Hydrograph Analysis

The time series diagram of the level of piezometer wells in the region from 2015-2019 is also shown as a groundwater interpolation map using the Kriging method to show groundwater changes.

2.2. Geographical Balanced Regression

Moran's index is an instrument in spatial self-correlation analysis that analyzes the pattern of distribution of features in space with simultaneous consideration of location and the value of the desired feature.

3. Results

The results of processing on the images show subsidence of about 24 cm in the studied area "Fig. 2". In order to study subsidence and its impact on the extraction of groundwater reserves in the part of Shabestar plain that has higher subsidence event has been selected as the studied area. The center of Shabestar and Tasuj plain has experienced the most subsidence and other areas have witnessed the occurrence of this phenomenon to a lesser extent.
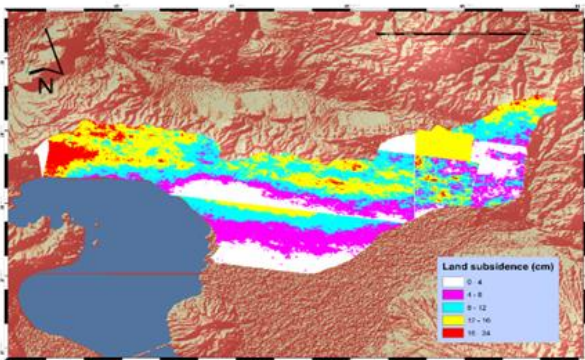

Figure 2. Map of Shabestar plain subsidence

The research tries to find a relationship between exploitation of water from existing wells and the phenomenon of subsidence. "Fig. 3" shows the distribution of water exploitation wells and the level of groundwater. The highest density of exploitation wells is observed in the center of the region located in the western parts of the studied area "Fig. 3".

Spatial analysis of these two parameters was performed by having a subsidence density map and changes in water level. Examination of these changes confirmed the existence of significant clustering in the area. Clusters with high values correspond to changes in water level shifted with the occurrence of subsidence and clusters with low values confirm the slight correlation of changes in level with the occurrence of subsidence "Fig. 4".
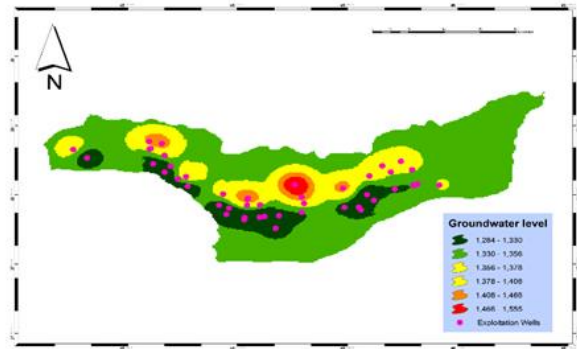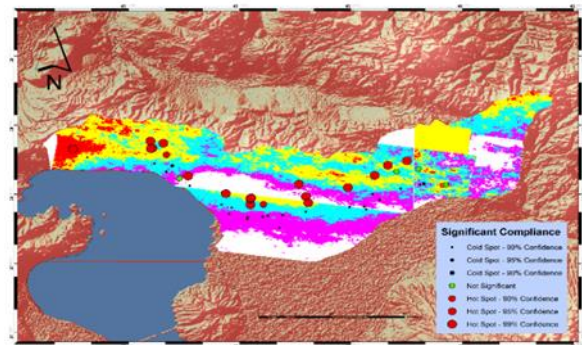

Figure 3. Groundwater water level map

Figure 4. Adaptation map of groundwater level changes and subsidence occurrence density

This analysis confirmed the Moran index of clustering subsidence under the influence of water changes in the studied area. The closer Moran index to one depicts the stronger cluster pattern. The results of the analysis of the present research indicated 0.98 for Moran index. On the other hand, the high standard score of Z and the low value of P-VALUE confirm the strong correlation between the studied elements, which in the present analysis are 477 and 0, respectively "Fig. 5".

Global Moran's I Summary	
Moran's Index:	0.987086
Expected Index:	-0.000044
Variance:	0.000004
z-score:	477.593058
p-value:	0.000000

Figure 5. Moran index Processing

4. Discussion

Interferogram of Sentinel A1 images with coherence values of 0.2 and base line 82 was provided. The results of InSAR analysis showed that the highest amount of subsidence is about 24 cm, which occurred in 2015-2019. Groundwater level in relation to the results of subsidence of Shabestar-Sufiyan plain indicated the plain subsidence in parts where the use of groundwater and the density of exploitation wells in the region and the amount of drought and subsidence in these areas have been reported.

According to the region climate, the groundwater level fluctuations used by farmers in this area with agricultural land covers, irrigated agricultural lands and gardens around the area in the villages of Chelekhaneh Oliya, Ali Akbar Lou, Cheshmeh Kanan, Ghezeljeh, Cheshmeh Kanan Station, Gholmansarai and Sahlan Customs are important factors in land subsidence.

5. Conclusion

In recent decades, it has experienced population growth along with agricultural development and has the highest subsidence of 24 cm, which can be imaged from the Sentinel A1 satellite with v-v bands in summer, which is the best result considered for accurate monitoring of the ground by InSAR radar interferometry. Low precipitation in recent years and successive droughts, resource constraints, improper irrigation methods in the agricultural sector in the studied area along with inappropriate cultivation pattern have led to excessive digging of water wells in the area. This subsidence, which is mostly seen in agricultural lands, has endangered the expansion of sinkholes, lands and villages of Shabestar and Tasuj plains and by destroying agricultural and garden lands, destroying roads and communication and service facilities and trapping livestock have influenced the lives of the residents of this area and have other negative effects that require sustainable and principled management of resources and awareness of managers in this area for solving the problem of crises and basic planning of the area.

References

Chen, C., Wang, C., Chen Kuo, L. (2010). Correlation between groundwater level and altitude variations in land subsidence area of the Choshuichi Alluvial Fan. Taiwan Engineering Geology 115:122–131.

Clement, M., Kilsby, C., & Moore, P. (2018). Multi-temporal synthetic aperture radar flood mapping using changedetection.J. Flood Risk Manag, 11, 152–168.

Dai, K., Li, Z., Tomás, R., Liu, G., Yu, B., Wang, X., Cheng, H., Chen, J., & Stockamp, J. (2016). Monitoring activityat the Daguangbao mega-landslide (China) using Sentinel-1 TOPS time series interferometry. Remote Sens. Environ, 186, 501–513.

Daniel, R., Maisons, C., Carnec, S., Le Mouelic, C., Kingands, H. (2003). Monitoring of slow ground deformation by ERS radar interferometry on the Vauvert salt mine (France) Comparison with ground-based measurement. Remote Sensing of Environment, 88(4): 468-478.

Galloway, D. L., Hudnut, K. W., Ingebritsen, S. E., Philis, S. P., Peltzer, G., Rogez, F., Rosen, P. A. (1998). Detection of aquifer system compaction and land subsidence using interferometric synthetic aperture radar, Antelope valley, Mojave Desert, California, Water Resour. Res., 34: 2573-2585.

Gatelli, F., Monti Guarnieri, A., Parizzi, F., Pasquali, P., Prati, C., & Rocca, F. (1994). The wavenumber shift in SARinterferometry.IEEE Trans. Geosci. Remote Sens., 32, 855–865.

Haykin, S. (2007). Adaptive Filter Theory, 4th edition, PearsonEducation Inc.

Ishitsuka, K., Tsuji, T., & Matsuoka, T. (2012). Detection and mapping of soil liquefaction in the 2011 Tohoku earthquakeusing SAR interferometry.Earth Planets Space, 64, 1267–1276.

Karimzadeh, S., & Ahmadi, F. (2013). Using Advanced Space-borne Radar Technology for Detection and Measurement of Land Subsidence and Interseismic Slip Rates, the Case Study: NW Iran.

Ketelaar, V. B. H. (2008). Satellite Radar Interferometry Subsidence Monitoring Techniques. Vol, 14. Netherlands. Springer Science.

Lu, C. H., Ni, C. F., Chang, C. P., Yen, J. Y., & Chuang, R. Y. (2018). Coherence difference analysis of Sentinel-1 SARinterferograms to identify earthquake-induced disasters in urban areas.Remote Sens, 10, 1318.

Motagh, M., Djamour, Y., Walter, T. R., Wetzel, H. U., Zschau, J., Arabi, S. (2006). Land subsidence in Mashhad Valley, northeast Iran: results from InSAR, levelling and GPS. Geophysical Journal International, 1-9.

Raucoules, D., de Michele, M., & Aunay, B. (2020). Landslide displacement mapping based on ALOS-2/PALSAR-2data using image correlation techniques and SAR interferometry: Application to the Hell-Bourg landslide.Geocarto Int., 35, 113–127.

Sun, H., Zhang, Q., Zhao Yang, Ch., Sun, Q., & Weiran, Ch. (2016). Monitoring Land Subsidence in the southern part of the lower liaohe plain,China with a multitrack PS-InSAR technique.

Twele, A., Cao, W., Plank, S., & Martinis, S. (2016). Sentinel-1-based flood mapping: A fully automated processingchain.Int. J. Remote Sens., 37, 2990–3004.

USGS (2014). Land Subsidence, The USGS Water Science School,online.

Vietmeier, J., Wagner, W., & Dikau, R. (1999). Monitoring moderate slope movements (landslides) in the southernFrench Alps using differential SAR interferometry. In Proceedings of the Fringe 1999 Workshop: AdvancingERS SAR Interferometry from Applications Towards Operations, Liège, Belgium, 10–12 November; Volume 99, pp. 10–12.

Walters, R. J., Holley, R. J., Parsons, B., & Wright, T. J. (2011). Interseismic strain accumulation across the North Anatolian Fault from Envisat InSAR measurements. Geophysical Research Letters, VOL. 38.

Wright, T., Parsons, B., & Fielding, E. (2001). Measurement of interseismic strain accumulation across the North Anatolian Fault by satellite radar interferometryGeophysical Research Letters, 28, NO. 10, 2117-2120.

Zebker, H. A. (1992). Decorrelation in interferometric radar echoes. IEEE Trans. Geosci. Remote Sens. 30,950–959.